# NUMERICAL AND EXPERIMENTAL ANALYSIS OF A SAVONIUS-STYLE WIND TURBINE OPERATING AT LOW WIND SPEEDS

A project report submitted as per the requirement for the completion of the B.Tech Project (MIN-400B)

by Putluru Deshik Reddy (18119026) Kota Chanikya Venkata Sai Haranadh (18117045) Kuldeep Sharma (18113076)

Under the guidance of **Prof. Sushanta Dutta** 



MECHANICAL AND INDUSTRIAL ENGINEERING DEPARTMENT INDIAN INSTITUTE OF TECHNOLOGY ROORKEE ROORKEE (247667), INDIA

Date of Submission: 15-04-2022

Candidate's Declaration

I hereby declare that the work carried out in this dissertation titled, "Numerical and

Experimental Analysis of a Savonius-Style Wind Turbine operating under low wind

speeds", is presented on behalf of partial fulfilment of the requirements for the award

of the degree of "Bachelor of Technology" in Mechanical Engineering submitted to the

Department of Mechanical and Industrial Engineering, Indian Institute of Technology

Roorkee (India), is an authentic record of my own work carried out during August 2021

to April 2022 under the supervision of Professor Sushanta Dutta, MIED, IIT Roorkee.

I have not submitted the record embodied in this report for the award of any other

degree in any other institute or university.

Putluru Deshik Reddy

18119026

Kuldeep Sharma

18113076

Kota Chanikya Venkata Sai Haranadh

18117045

Date: April 15,2022

Place: IIT Roorkee

## **Certificate**

This is to certify that the report submitted by Mr.PUTLURU DESHIK REDDY, Mr.KOTA CHANIKYA VENKATA SAI HARANADH and Mr.KULDEEP SHARMA on "Numerical and Experimental Analysis of a Savonious Style Wind Turbine Operating at Low Wind Speeds" in a partial fulfilment of the B.Tech Project (MIN-400B), is an authenticated record of their project work which they have satisfactorily completed under my supervision. However, it does not endorse the statements full or partially made within this report.

Signature:

Supervisor Name: Dr. Sushanta Dutta

## Acknowledgement

This project would not have been possible without the contributions of several people. To all of these people, we would like to express our gratitude.

First and foremost, we would like to express our deep gratitude and heartfelt thanks to our supervisor, Dr. Sushanta Dutta, Professor, Mechanical and Industrial Engineering Department, IIT Roorkee, for guiding us throughout the project and providing us with the best resources. We would like to thank him for providing us with an opportunity to work in this emerging field of research of vertical axis wind turbines. His expertise in fluid mechanics have provided us with the opportunity to gain knowledge and learning experience in the meticulous design of the wind turbine and the practical experimentations. Without his guidance and persistent help, this dissertation would not have been possible.

We are grateful to Tinkering Lab, IIT Roorkee who provided us with the 3d prints of all the required designs of models, which laid the very foundation of the project. We are also thankful to the Flow Control and Turbine Research Laboratory, Department of Mechanical and Industrial Engineering, to help us conduct the experimental research on the wind turbine.

A word of gratitude to Mr. Vikas Sharma, whose regular guidance and support was very helpful during the course of this project work. His knowledge and experience in the fluid mechanics field was very helpful. We are also thankful to our institute to provide us with the platform to do this research. Finally ,we would like to thank our parents and friends for their never ending support and encouragement.

## Contents

Lis	st of Figures	6
1	Introduction           1.1 Motivation            1.2 Problem Statement            1.3 Objectives	8 8 9 10
2	Literature Review	10
3	Theory	11
4	CAD Modeling	14
5	Numerical Simulation 5.1 Governing Equations	14 15 15
6	First Case 6.1 Results	<b>16</b> 18
7	Parametric Analysis	20
8	Spline Optimization 8.1 Methodology	<b>21</b> 21 23
9	Experimentation  9.1 Prototype	24 25 25 25
<b>10</b>	Gust Protection Mechanism	30
11	Scaling wind turbines	32
12	Conclusion	32
13	References	34

## **List of Figures**

1	Savonious turbine	8
2	Global Energy consumption 2000 to 2020	9
3	Engagement of wind flow with turbine blades	12
4	Schematic diagram of Savonius Rotor	13
5	Cross section and splines of the sketch	14
6	Mesh and setup of 2D validation test case	16
7	Boundary conditions for first simulation case	17
8	Meshing in section view	18
9	Velocity streamlines for initial simulation	19
10	Perssure contours for initial simulation model	19
11	Different AR CAD models for parametric analysis	20
12	Coefficient of moment vs Aspect Ratio	21
13	Spline angle parametrization	22
14	Spline angle parametrization at other end	22
15	Pressure contours for optimized model	23
16	Velocity contours for optimized model	24
17	Schematic of wind tunnel at Flow-CTRL	25
18	Fixture of turbine to wind tunnel from top-side view	26
19	Measurement of turbine rpm using tachometer	26
20	Wind Turbine rpm variation with wind speed in tunnel	27
21	Voltage difference generated vs wind speed in tunnel	28
22	Wake Rake Theory	28
23	Setup for Rake method	29
24	Plot of pitot readings/Velocity profile	30
25	Schematic representation of gust protection plan	31
26	Closing of turbine on heavy gust flow	31

## **Abstract**

Wind energy is one of the major forms of renewable energy resources found abundantly on our planet. Wind power is sustainable and due to lack of fossil fuels, the need for wind power to generate electricity is increasing day by day. Among the two types of wind turbines, vertical axis wind turbines are most often used for domestic purposes. The performance of savonious style wind turbine depends on overlap ratio and the shape characteristics. In this project, we aim to optimise the geometrical parameters of an SSWT(Savonius Style Wind Turbine) blade design such as aspect ratios, blade profile & overlap distance to increase the power conversion efficiency parameter coefficient of moment  $(C_m)$ . In each design iteration, the airflow behaviour will be analysed at low wind speeds usually around 0.5-5 m/s using ANSYS Fluent software. Also, a 3D printed prototype of the final design will be fabricated and experimented with using the wind tunnel facility at the Flow CTRL laboratory. Finally, a mechanism for auto-stopping the turbine in case of severe operating conditions such as wind gusts will be proposed.

## **Nomenclature**

#### **Alphabetical Letters**

 $C_d = \mathsf{Coefficient}$  of drag

 ${\it Re}={\it Reynolds}$  number

D = Diameter of the turbine

 $U_{\infty} =$  Free stream velocity of air

 $C_m = \mathsf{Coefficient}$  of moment

### **Greek Symbols**

 $\omega = Angular velocity$ 

 $\theta = Angleofattack$ 

 $\eta = Efficiency$ 

 $\sigma = Stress$ 

#### **Abbreviations**

SSWT = Savonius-Style Wind Turbine

VAWT = Vertical Axis Wind Turbine

SST = Shear Stress Transport

CTRL = Control Turbine and Research

Laboratory

CAD = Computer Aided Designing

CFD = Computational Fluid Dynamics

PIV = Particle Image Velocimetry

HAWT = Horizontal Axis Wind Turbine

### 1 Introduction

Savonius Style Wind Turbine (SSWT) is a vertical axis wind turbine that usually consists of two or three rotor blades. It is a drag-based wind turbine. It is one of the simplest designs which can be easily manufactured and used for small-scale power generation.

The advantage of these turbines is that they start rotating at even low wind speeds. So these turbines can be installed at ground level heights and also at rooftops in residential urban areas. However, it has a lower efficiency than other horizontal axis turbines because of its drag-induced torque nature. In this project, we focussed on a specific design of an SSWT to study and improve its performance.

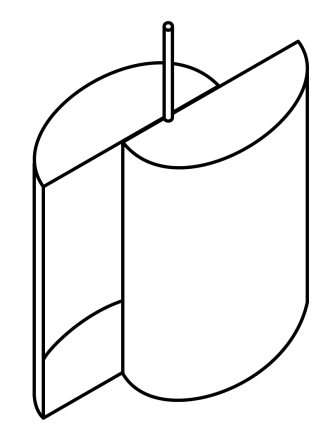


# **Figure 1.** Savonious turbine

#### 1.1 Motivation

Renewable Energy Development has become a topic of interest for many researchers nowadays. Even though renewable energy is a source of power generation, its contribution to

the global energy chart is still low. As per Figure.2, the three major sources of energy are coal, oil, and natural gas. Renewable energy, which comprises hydro and other renewables, is still running behind. According to IEA Global Renewable Energy Review 2021, the share of renewables in global electricity generation in 2020 is only 29%. However, in recent times, due to the decline of fossil fuel resources and simultaneously the continuous research and development in the renewable areas, the growth of the renewable energy usage for electricity generation is increasing at a fast pace. This is evident from the Figure.2, where there is an exponential increase in the other renewable sources which include wind, biomass, geothermal, etc. Wind energy, being one of the most used renewable energies, has got some very good advantages over other renewables. Its cost per KWH is lower than that of solar [1], which represents that it is cost efficient to extract electricity from wind rather than solar. Wind energy is mainly derived using wind turbines. The majority of the power generation from wind comes from the Horizontal Axis Wind Turbines (HAWT) that are commercially installed as wind farms. The Vertical Axis Wind Turbines (VAWT) were not so popular earlier for

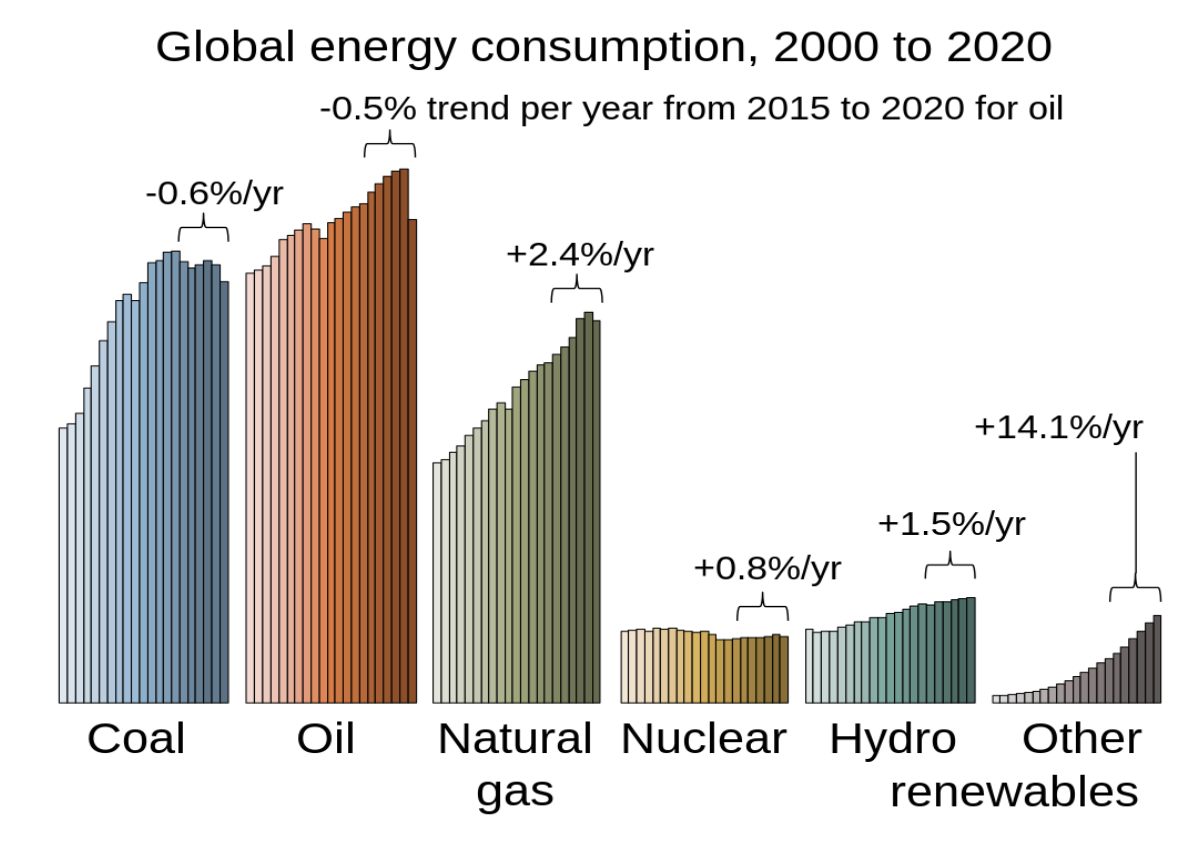


Figure 2. Global Energy consumption 2000 to 2020

their relatively low efficiencies[2]. However, they have become popular lately due to their advantages for small-scale purposes over HAWTs. In residential areas (mainly urban), to capture wind energy it is not possible to set up huge horizontal windmills due to their installation requirements and strict guidelines. Whereas VAWTs offer fewer restrictions on the size and wind speeds. They can be operated at low wind speeds also, which is the case in urban and suburban areas. Moreover, VAWTs are independent of wind direction, unlike HAWTs which have a strong directional dependency for greater efficiency. So it is necessary to understand the VAWTs much better and improve their efficiencies for the better extraction of wind energy in residential areas and for small-scale purposes.

#### 1.2 Problem Statement

The main drawback of the SSWTs is their poor performance and lower efficiencies. This is due to the following reasons:

- 1. These turbines experience negative torque on one blade and positive torque on the other blade which decreases the net output torque and accordingly the power.
- 2. Drag based turbines are aerodynamically less efficient in extracting the available wind energy.
- 3. At heavy wind speeds (Gust conditions), these turbines experience high mechanical loads and may undergo physical damage due to no protecting mechanism.

Due to all these drawbacks, SSWTs are running little behind the conventional WTs available in the market. As future engineers, it is our duty to focus on such capable technologies and improve their value.

#### 1.3 Objectives

This project focuses on one specific design of SSWT which resembles a tree leaf. The objectives of this project are,

- 1. to optimise the blade design of the given SSWT using CAD and numerical simulations.
- 2. to test the prototype in the wind tunnel and check the resulting performance.
- 3. to design a mechanism for protecting the turbine blades from the gust conditions.

The following sections discuss how the above mentioned objectives are achieved in this project. But before that a complete detailed review of the literature in this domain is presented in the next section.

### 2 Literature Review

The Savonius Wind Turbine is named after S.J Savonius, who in 1924 proposed a rotor design with a cylinder open to the atmosphere. The two halves of the cylinder arranged in an S shaped manner is the "Savonius rotor" which is still known today. Even though its efficiency is low (around 31%, as claimed by Savonius), the simplicity in its design is what attracted many researchers. A number of studies were performed on the conventional Savonius style rotor for improving the efficiency. Fujisawa et al. in their flow visualisation experiments in 1992 showed that the negative torque on the returning blade is limiting the efficiency of the turbine[3]. To diminish this negative

torque, researchers used various design attributes such as deflectors, guide vanes, nozzles, curtains etc. They were added upstream to the returning blade to outbalance the negative torque acting [4][5][6][7]. Deflectors and guide vanes work for both the blades. Unlike curtains, they were used to direct the flow to the advancing blade besides restricting the flow to attack on the returning blade. But all these made the rotor design very complex and directionally dependent which was not encouraging. So to stick with the advantages of the Savonius style rotor (simplest design and operable at low wind speeds) researchers started investigating the blades' profiles, shape, and size to enhance the performance. Nobuyuki et al. studied the effect of overlap ratio on the turbine's performance. A small overlap ratio (0.15) gives better recirculation and aerodynamic advantage than the large overlap ratios[8]. Mahmoud et al., studied multiple parameters experimentally in the wind tunnel. They stated that the two bladed rotors have a significant advantage over the three bladed ones. They also performed experiments on multi staged turbines. The results showed that double staged turbines give much better power coefficient than the single staged ones[9]. Numerical Methods were also used to predict the performance of different new designs of the turbine. Dobreva and Massouha, used CFD methods to study the unsteady behaviour of the turbine (vortex shedding, etc). Turbulence modelling involving k-  $\omega$ model was used in their simulations. They validated his numerical results with the PIV (Particle Image Velocimetry) experimental results[10]. PIV experiments result in a detailed flow behaviour around the testing model using optical techniques. To improve the numerical simulations predictions, Nasef et al. tested multiple turbulence models and obtained a detailed comparison between them. Of all, the SST k- $\omega$  turbulence model standed out to be the best one for simulating the Savonius style turbines[11].

The studies from all these researches laid a strong foundation for us to move forward in this project.

## 3 Theory

This section discusses the physics behind the wind turbine which is responsible for the power generation. As shown in the Figure.3, wind having uniform velocity travels towards the turbine which is mounted vertically. The turbine rotor consists of two

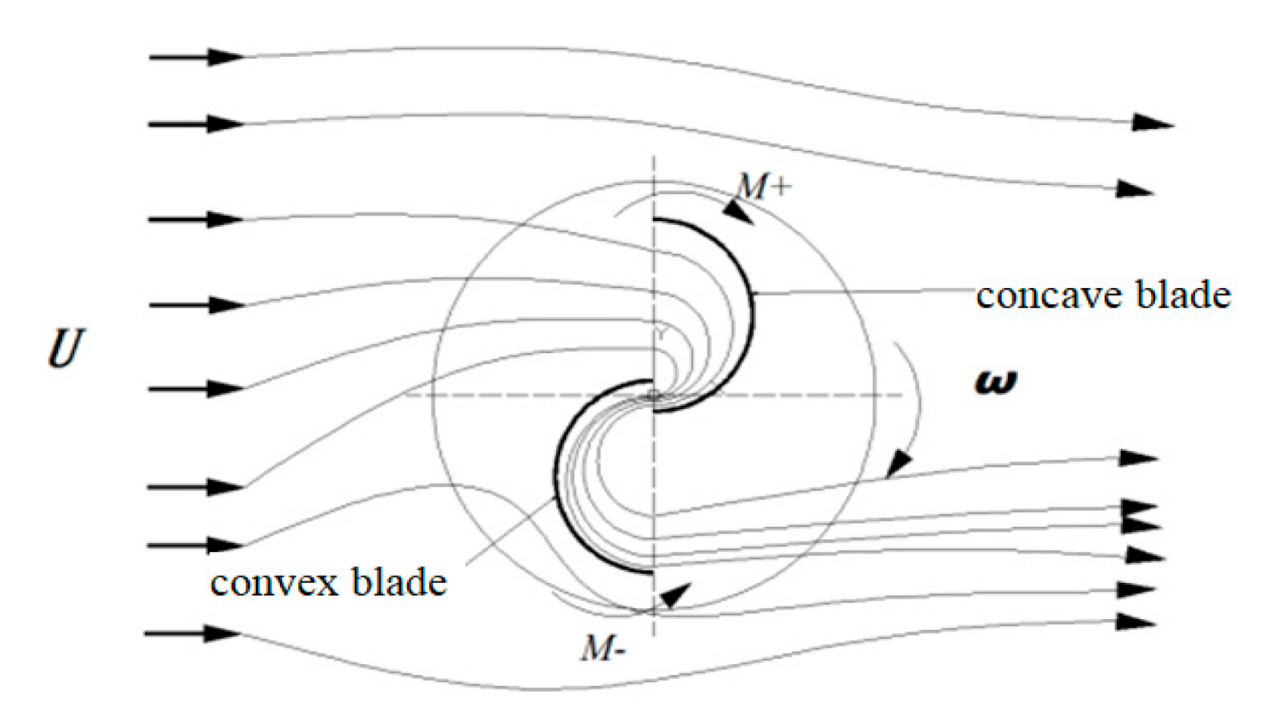


Figure 3. Engagement of wind flow with turbine blades

blades and each blade has one concave side and one convex side. Almost at every instant, one side of each blade faces towards the wind. The blade which has its concave side facing the wind is called the advancing blade at that instant. Similarly the blade with its convex side facing the wind is called the returning blade.

Wind hits both the blades and gets deflected causing pressure differences across the blades. The two blades experience different pressure differences across them. It is because the concave side captures wind better than the convex side resulting in a large pressure difference for the advancing blade and a relatively small pressure difference for the returning blade. Due to the difference in the pressure differences, there is a net torque acting on the turbine in such a direction that the advancing blade moves along the wind and the returning blade moves against the wind. Now it may be apparent why the blades are named as advancing and returning respectively. To measure the performance of these turbines there are certain parameters that are important and are used frequently. Below are the definitions of all such parameters-

- 1. Coefficient of Moment,  $C_m$ : Torque generated  $\div 0.5 \rho U_{\infty}^2 D_r$
- 2. Coefficient of Drag,  $C_d$ : Drag Force  $\div 0.5 \rho U_{\infty}^2 A_f$

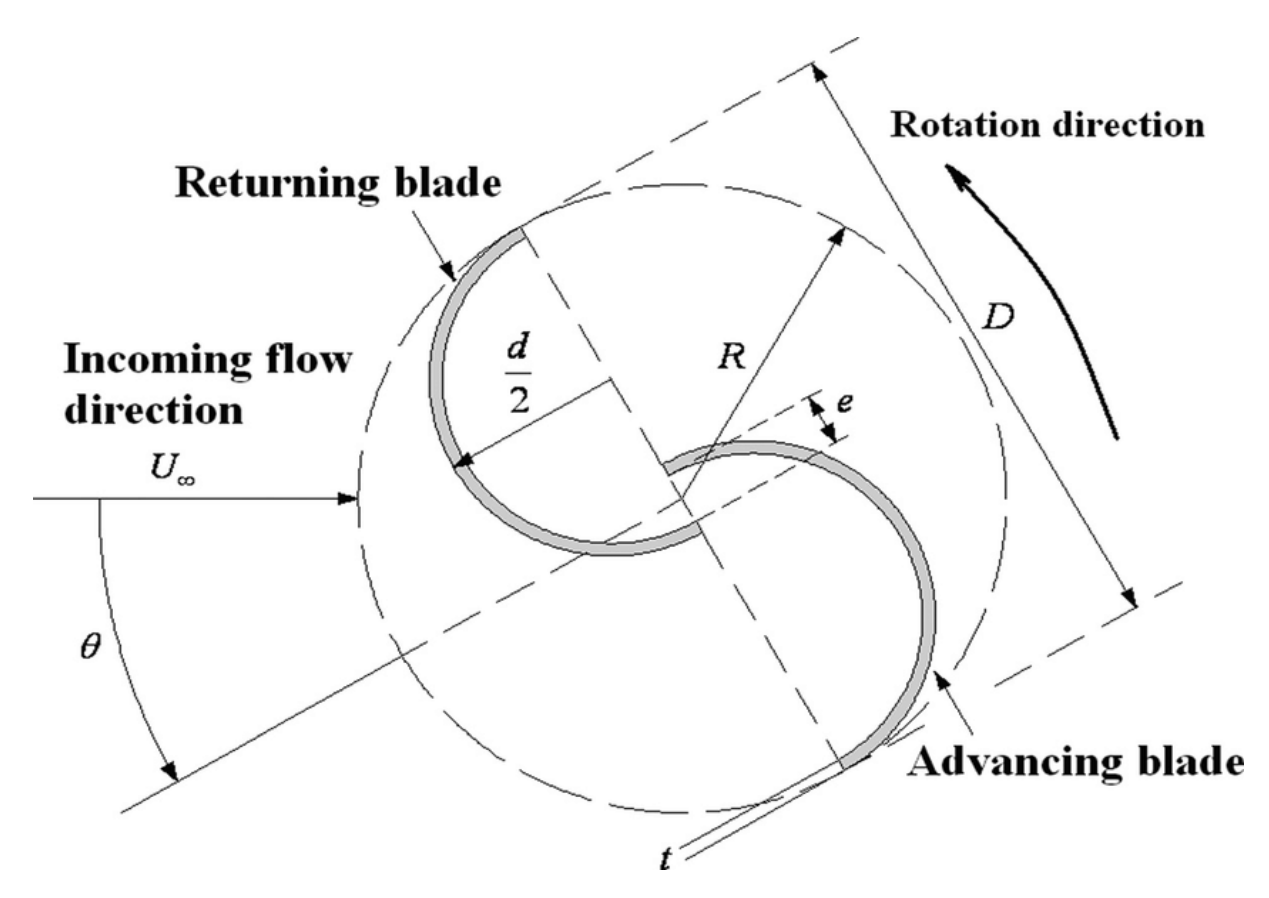
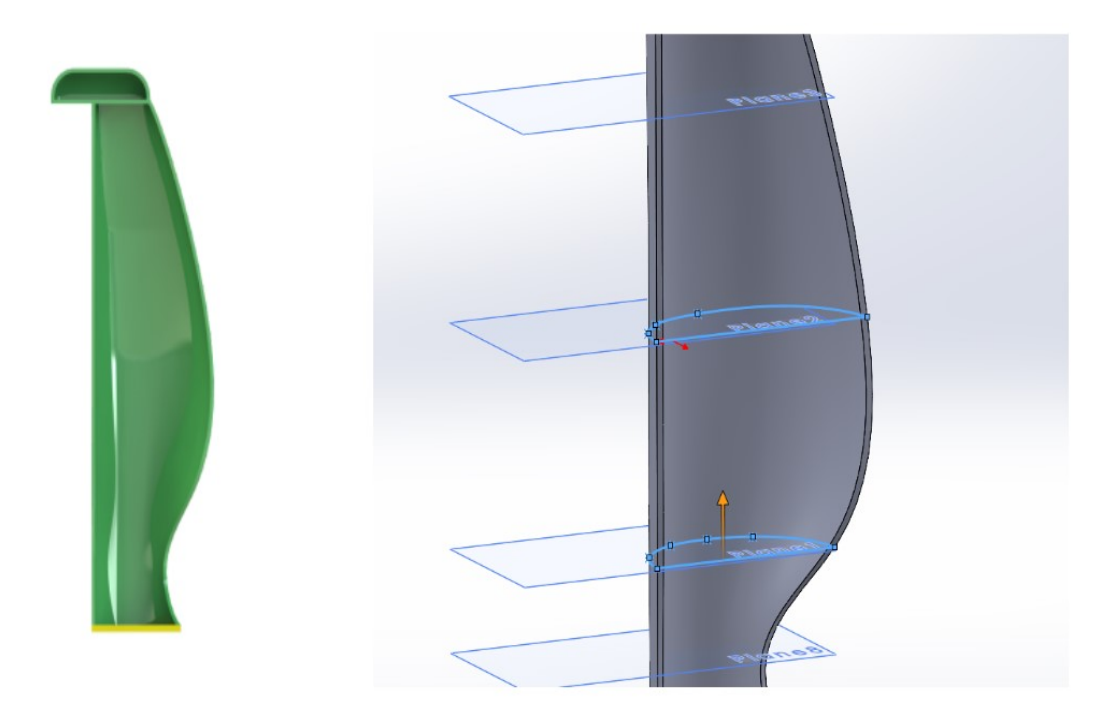


Figure 4. Schematic diagram of Savonius Rotor

3. Efficiency,  $\eta$ : Efficiency of turbine is measured by calculating coefficient of power,

$$C_p = \frac{Electricity \, produced \, by \, wind \, turbine}{Total \, Energy \, available \, in \, the \, wind}$$

where,  $A_f=$  Frontal Area  $D_r=$  Effective diameter of body with respect to rotating axis



**Figure 5.** Figure shows cross section sketches and splines at four planes. Later, lofted through 3D guide curves

## 4 CAD Modeling

As mentioned before, this project focuses on one specific design of SSWT, which mimics the leaf of a tree. It is not a commercially popular design as it is relatively new to the markets and also there were no prior reports produced on it. In this project we designed the turbine from scratch with the help of a few 2-D abstracts and drawings. As the design has multiple complex splines, we preferred to manually optimise by making multiple CAD models using Solidworks software. The designing phase is inspired from making of fairings, where multiple cross sections were made and then moulded to get the final shape. The initial geometry is very crudely designed, which is shown in Figure.5. The maximum height of the turbine is 730.5 mm, whereas the maximum chord-side length of the turbine is 273.2 mm. In the Figure.6, A clear display of geometry making is shown.

## 5 Numerical Simulation

To analyse the designed CAD model under testing conditions, numerical simulation methods were chosen before performing the experiments. For this ANSYS Fluent

was used because of its ease to parametrize and greater user interface. Due to the presence of adverse pressure gradients at blade tip, we added turbulence modelling to our simulation. From literature [11], it is found that the k- $\omega$  SST \* model is the best one to simulate this type of test cases.

#### 5.1 Governing Equations

The numerical wind flow simulation using ANSYS Fluent of the test case requires a mathematical model to solve the problem. Following are the governing equations which also includes k and Omega transport equations required for the turbulence modelling: \*

1. Continuity Equation

$$\frac{\partial \bar{u}_i}{\partial x_i} = 0$$

2. Momentum Conservation

$$\frac{\partial \bar{u}_i}{\partial t} + \bar{u}_j \frac{\partial \bar{u}_i}{\partial x_j} = \bar{f}_i - \frac{1}{\rho} \frac{\partial \bar{p}}{\partial x_i} + v \frac{\partial^2 \bar{u}_i}{\partial x_j \partial x_j} - \frac{\partial u_i^{\bar{i}} u_j^{\prime}}{\partial x_j}$$

3. Transport Equation for k

$$\frac{\partial k}{\partial t} + U_j \frac{\partial k}{\partial x_j} = P_k - \beta * k * \omega + \frac{\partial}{\partial x_j} [(v + \partial_k v_T) \frac{\partial k}{\partial x_j}]$$

4. Transport Equation for  $\omega$ 

$$\frac{\partial k}{\partial t} + U_j \frac{\partial k}{\partial x_j} = \alpha S^2 - \beta * \omega^2 + \frac{\partial}{\partial x_j} [(v + \sigma_\omega v_T) \frac{\partial k}{\partial x_j}] + 2(1 - F_1) \sigma \omega^2 \frac{1}{\omega} \frac{\partial k}{\partial x_i} \frac{\omega}{x_i}$$

#### 5.2 Framework

Before performing the actual simulations, a validation of flow over a cylinder is performed in ANSYS to check our methodologies and framework.

<sup>\*</sup>In our test case we used the revised model constants  $\sigma=1$ ,  $\sigma_w1=2$ ,  $\sigma_w2=1.17$ ,  $\gamma=0.44$ ,  $\beta_z=0.083, \beta_z=0.09$ 

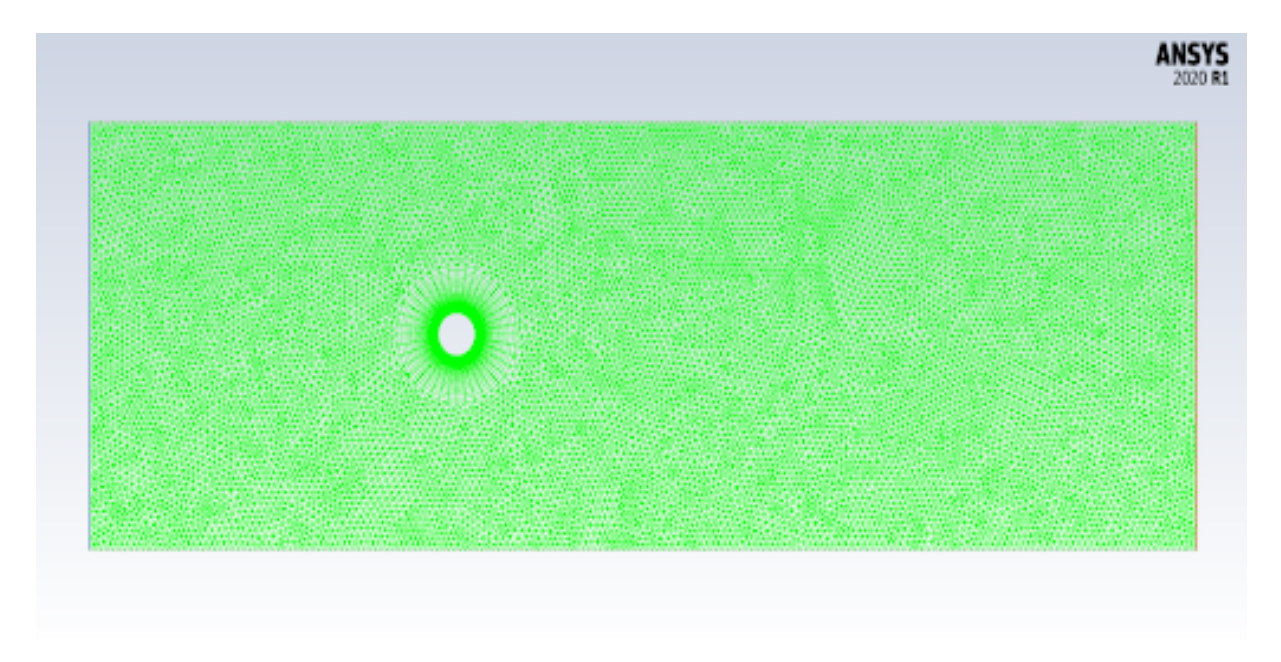


Figure 6. Mesh and setup of 2D validation test case

The same operating conditions as in the actual SSWT case were used. A cylinder of diameter 20cm is placed eccentric to the centre of a cubic enclosure. The fluid is assumed to be incompressible air with an inlet velocity of 5 m/s. The geometry and results are as shown below,

The results shown are close to the experimental results except at high Re and close at all points when compared with standard numerical simulations. This proves that the methodology and framework followed is accurate to use for further cases.

#### 6 First Case

As a first step after framework validation, we analysed the initially designed CAD geometry using Fluent software. The geometry was imported to DesignModeler software, followed by enclosure making. The turbine is static, which makes the analysis only shape dependent. So, the entire solid geometry was subtracted from the enclosure using a boolean feature. This turned into a single fluid domain with an obstacle in the interior region. A complete detailed boundary conditions and set up that was used in the Fluent is given in the table below,

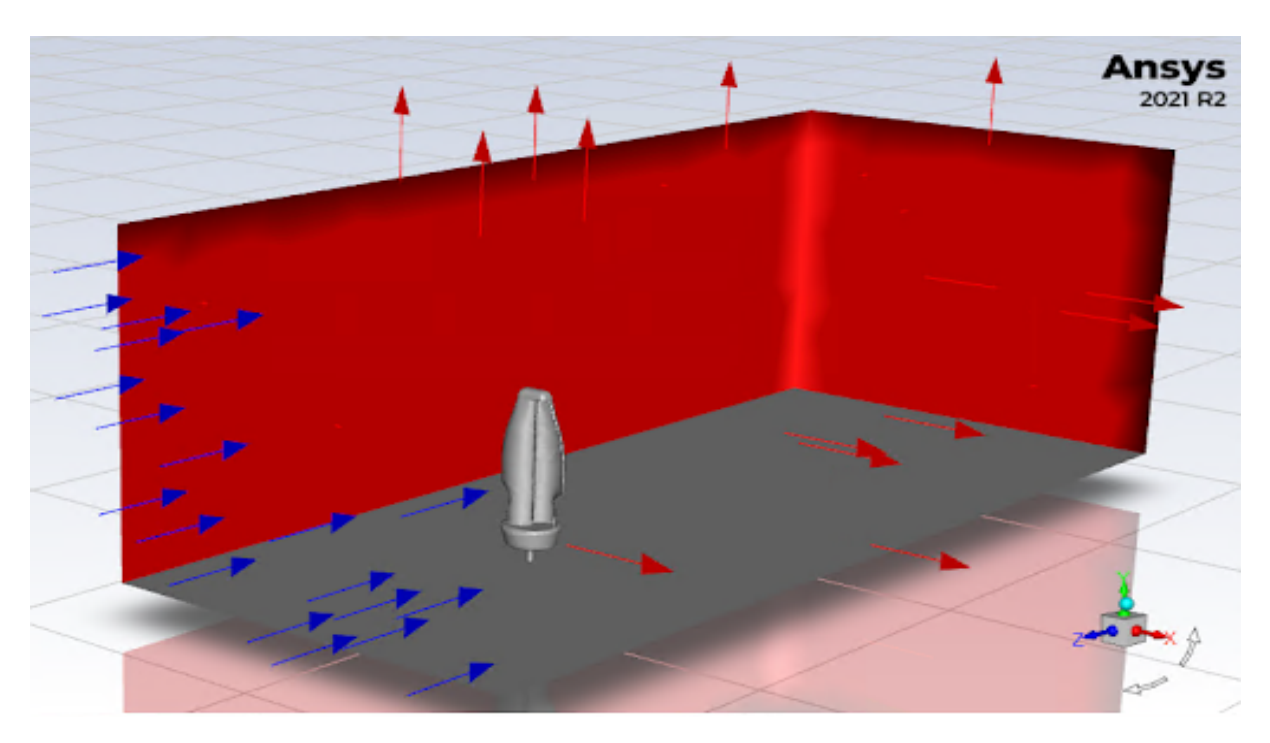


**Figure 7.** Boundary conditions for first simulation case, inlet velocity of 2 m/s is given with outlet as pressure outflow boundary type

Solver	3D, Pressure based	
Time Dependency	Steady	
Turbulence Model	$K ext{-}\omega$ SST	
Energy Equation	Off	
Fluid	Air at normal conditions	
Boundary Conditions	Inlet Velocity $= 5 \text{m/s}$ and Outlet: Pressure Outflow	

Due to high pressure gradients across the turbine boundary, meshing at those regions plays an important role in the accuracy of flow simulation results. A finer mesh was generated with 428659 elements and 78056 nodes, which included linear ordered tetrahedral and hexahedral elements. Ansys has a special feature "Adaptive Meshing" to refine the mesh at corners and edges. Inflation layers were added at the surface of the model, to capture the boundary layer effects. Following are a few calculations for calculating the specifications of inflation layers, [Calculations for inflation layer] The governing equations, presented in section 5.1, and boundary conditions (Table), together were solved iteratively until the solution converges. The Turbulent Kinetic Energy and Specific Dissipation Rate were solved with first order upwind schemes. Rhie-Chow distance based interpolation was employed for pressure-velocity coupling.

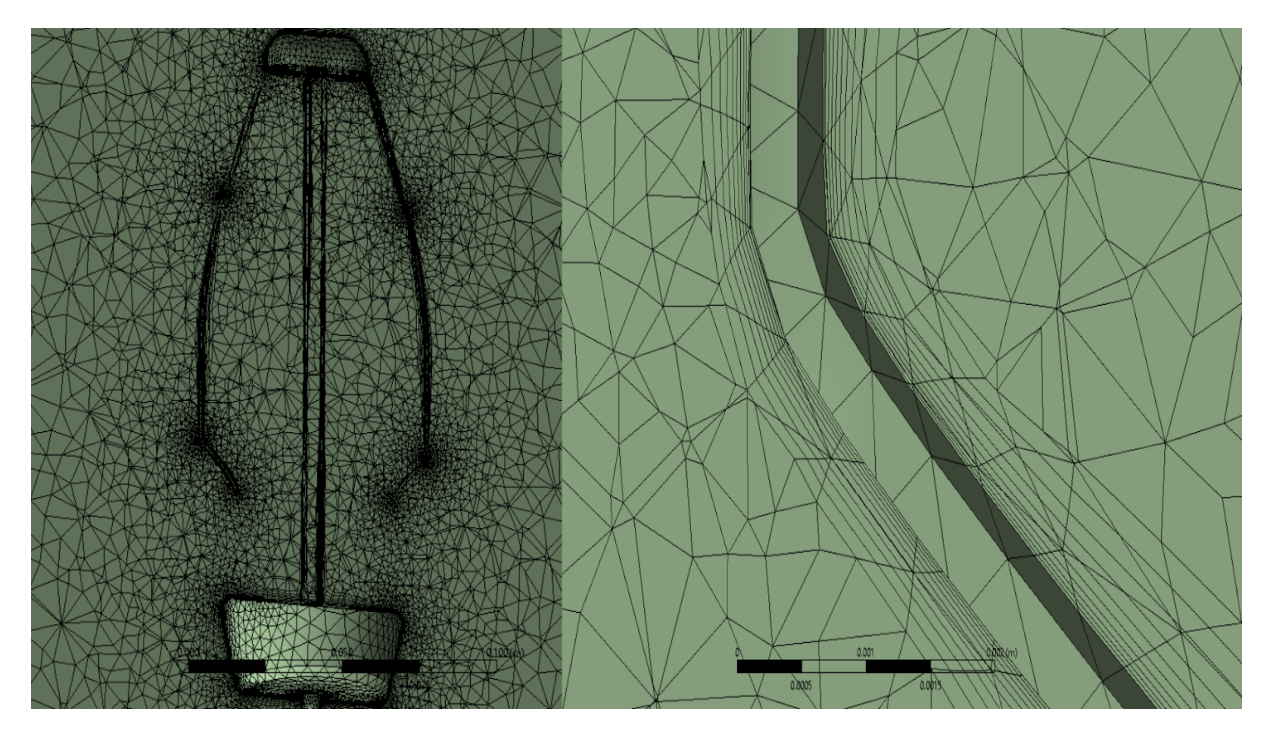


**Figure 8.** Unstructured meshing, mesh shows tetrahedral and hexahedral type cells . RHS shows inflation layers on the blade surface.

Reference values were computed from the inlet, and were used in calculating the Cd and Cm. The problem is initialised using boundary interpolation methods, where temperature, turbulence, and other parameters are automatically patched based on domain averaged values. The transient simulation is runned for 30s with each timestep of 1s and maximum of 40 iterations per timestep. The residual/convergence criteria is kept at  $10^-4$  for all variables, and  $10^-3$  for the continuity equation.

#### 6.1 Results

Below are the resultant streamlines and velocity contours. Before going to the physical quantities like Cm etc. there are few things which can be inferred from these contours.

- 1. There are very few number of streamlines (relatively) passing through the overlap region to the returning blade
- 2. Many streamlines are deflecting away from the tip edge of the blade.
- 3. Pressure discontinuities (adverse pressure gradients) are present near the overlap region.

From these it can be seen that there needs to be a thorough re-check and improvisations required in the design of the turbine, which will be presented in the upcoming sections.

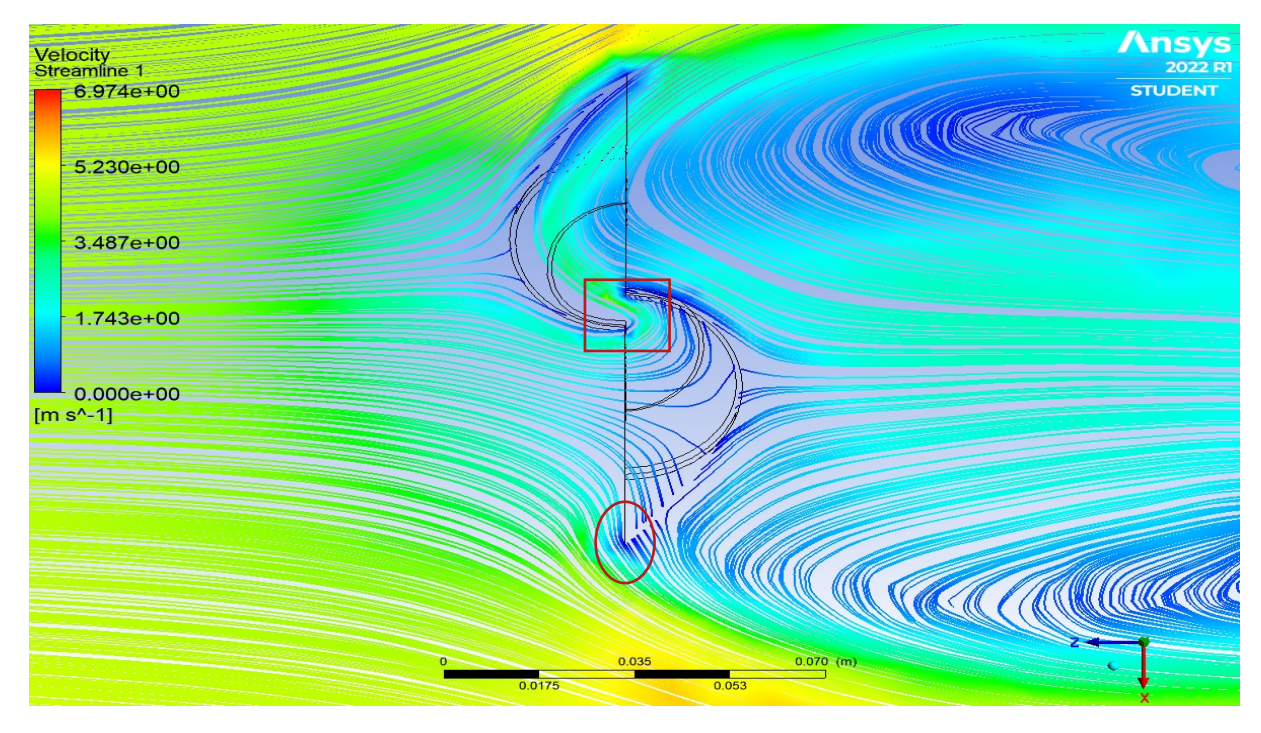


Figure 9. Velocity streamlines for initial simulation

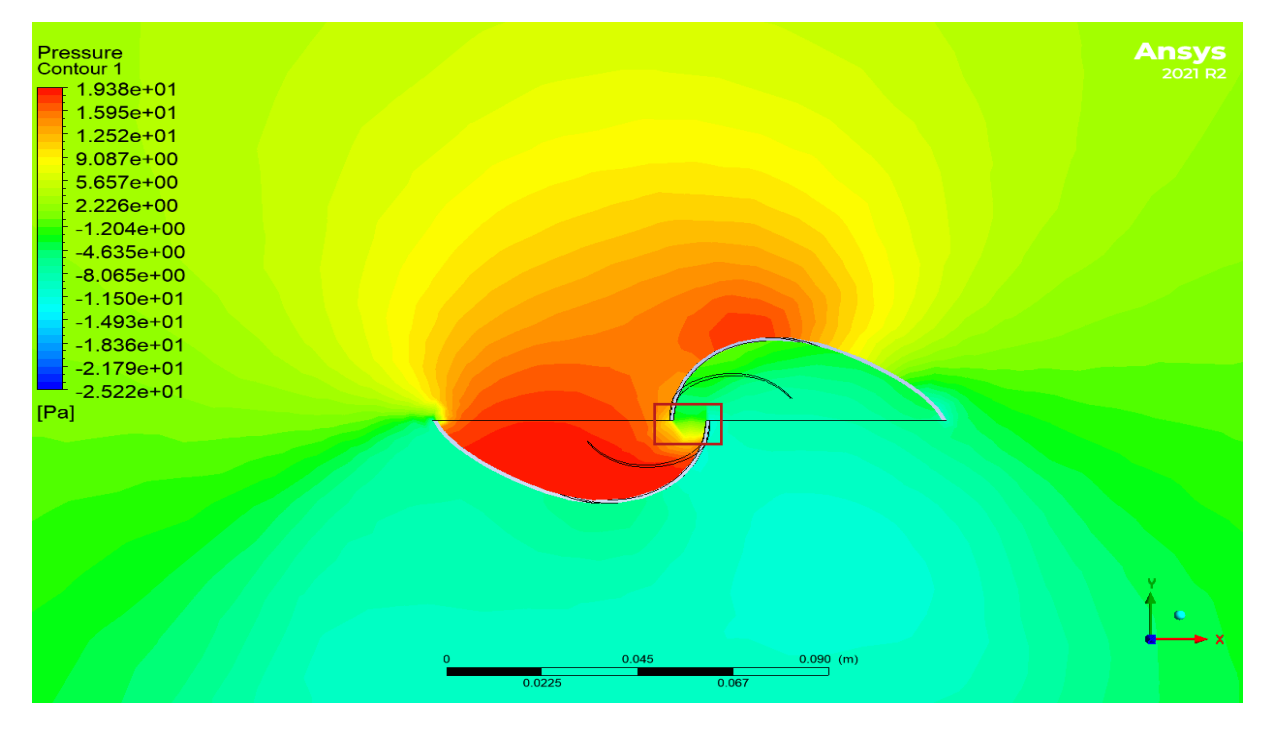


Figure 10. Perssure contours for initial simulation model

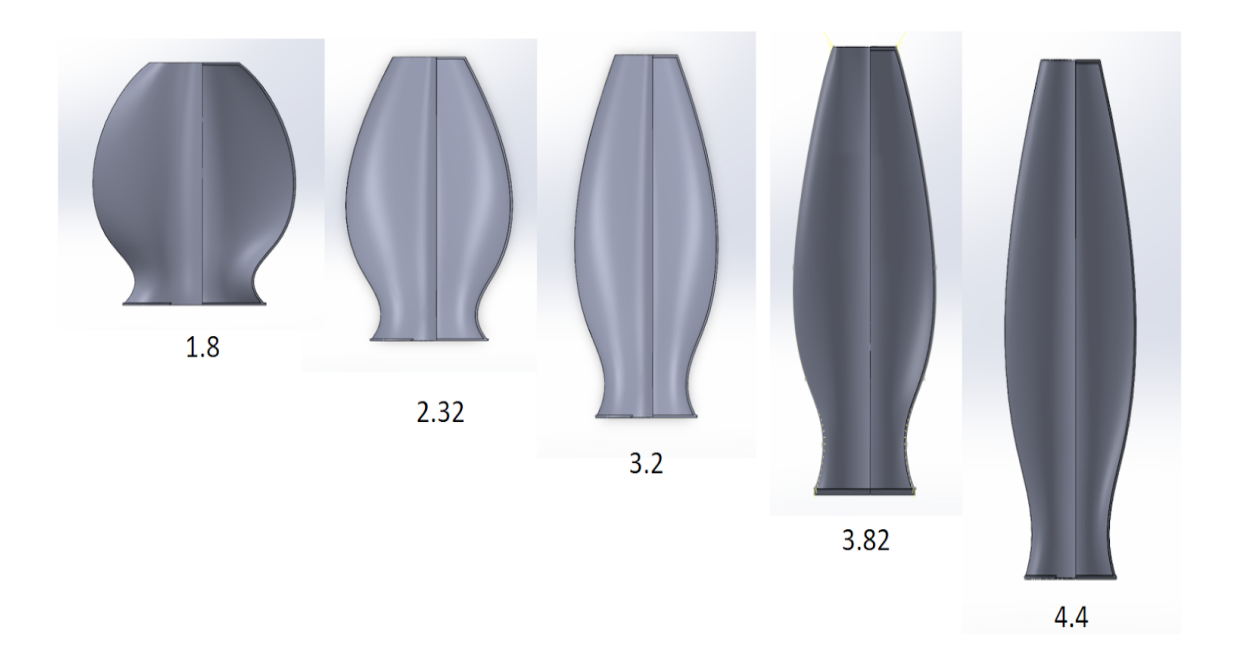


Figure 11. Figure shows different aspect ratio - CAD models made for parametric analysis

## 7 Parametric Analysis

As a part of the optimization, parametric analysis on the aspect ratio of the turbine was performed. Aspect Ratio (AR) is defined as the ratio of height of the blade to the maximum lateral distance of the blade. The geometry at this complexity is very difficult to be parameterized automatically/mathematically with respect to aspect ratios, thus manual analysis is preferred. We designed 7 models manually with different aspect ratios, keeping the frontal area constant. The spline opening and closing angles are kept constant for all the test cases. Aspect ratios of 1.4, 1.8, 2.32, 3.2, 3.35, 3.82, 4.4 are considered for the analysis and the results are represented in table and line plot (Figure.13)

The variation of Cm, which is desired to be high, significantly increased initially with aspect ratio, but there is no variation in Cm with respect to Aspect Ratio after 2.3. So, the AR-3.82 (first case) is kept unchanged for further optimization.

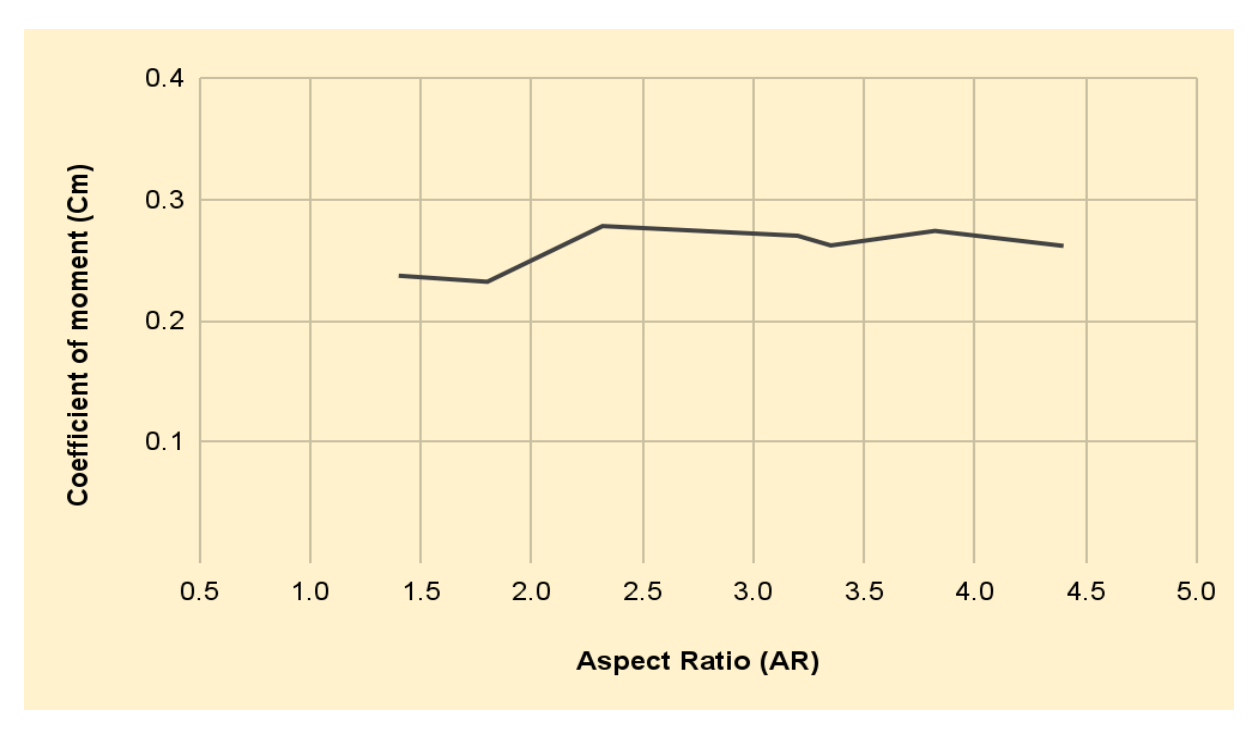


Figure 12. Coefficient of moment vs Aspect Ratio

## 8 Spline Optimization

From the inferences from first wind flow analysis, several adjustments were made in the geometry of the blade. One of the key flaws in our design was pressure discontinuities near the end tip and overlap tip. The streamline study shows that a significant number of streamlines deviating away from the blade end and overlap regions. Although optimizing the entire 3D shape is highly complex, and no commercial software/code is available, we simplified the optimization to spline<sup>†</sup> optimization. The splines in all the planes are to be shape optimized for better performance.

## 8.1 Methodology

As the blade itself is made of multiple cross-sectional planes, sketches and splines, we need to optimise the spline of the turbine. The ends and overlaps are parametrized keeping the main body/core of the spline unchanged. The following are steps for optimization,

1. A tangent line is drawn at the end fit point of the spline as shown in Figure.14 and 15

<sup>&</sup>lt;sup>†</sup>A spline consists of multiple control points and fit points through which are the key parameters that define its shape

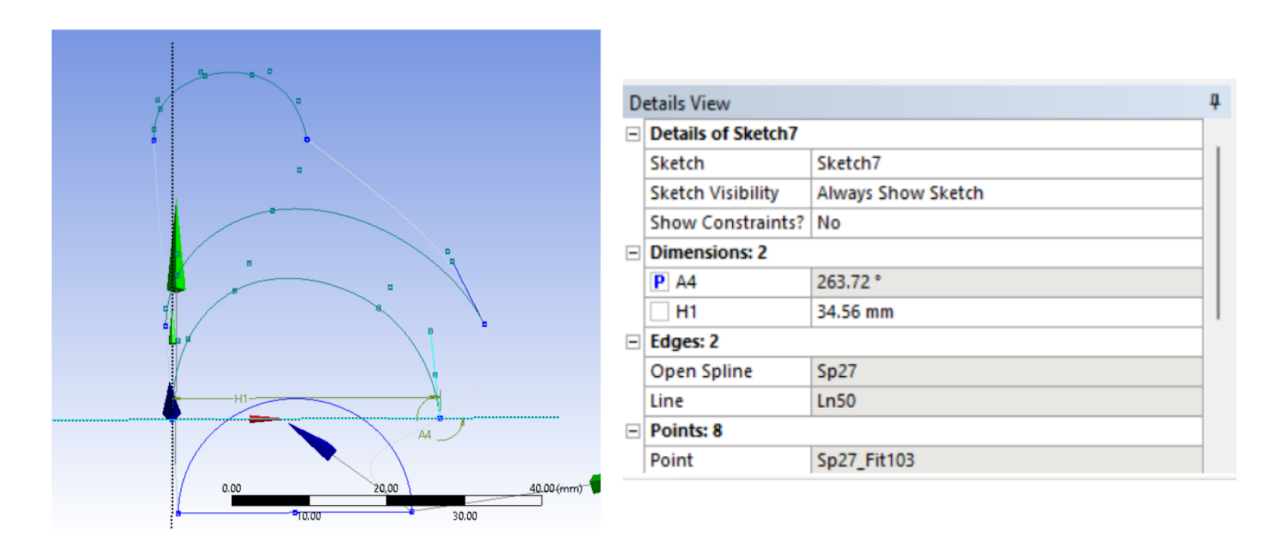


Figure 13. Figure shows the angle between tangent and horizontal line is parametrized

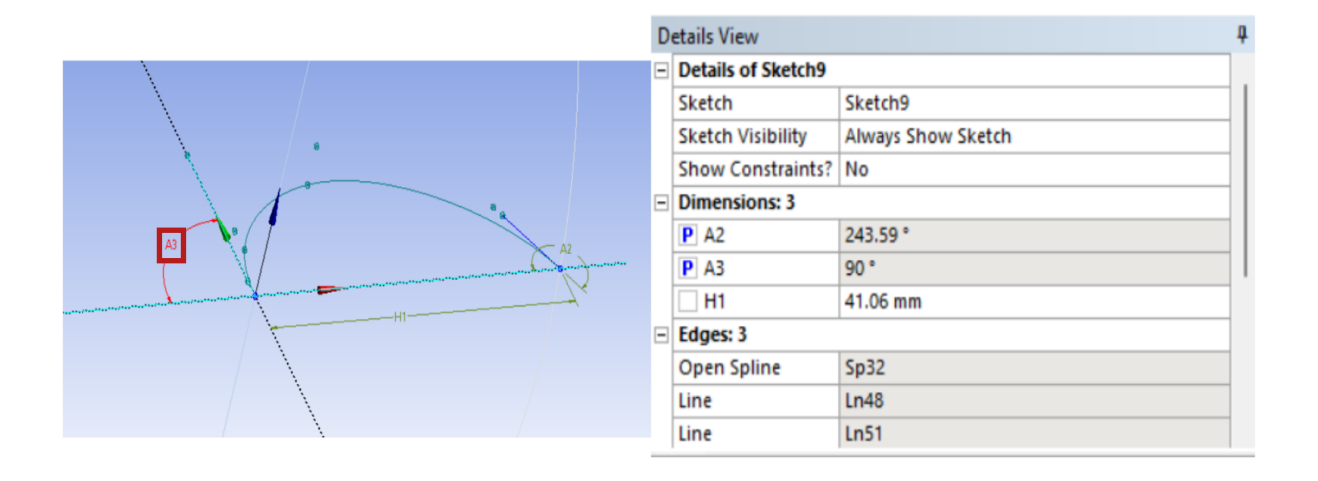


Figure 14. Spline angle parametrization at other end

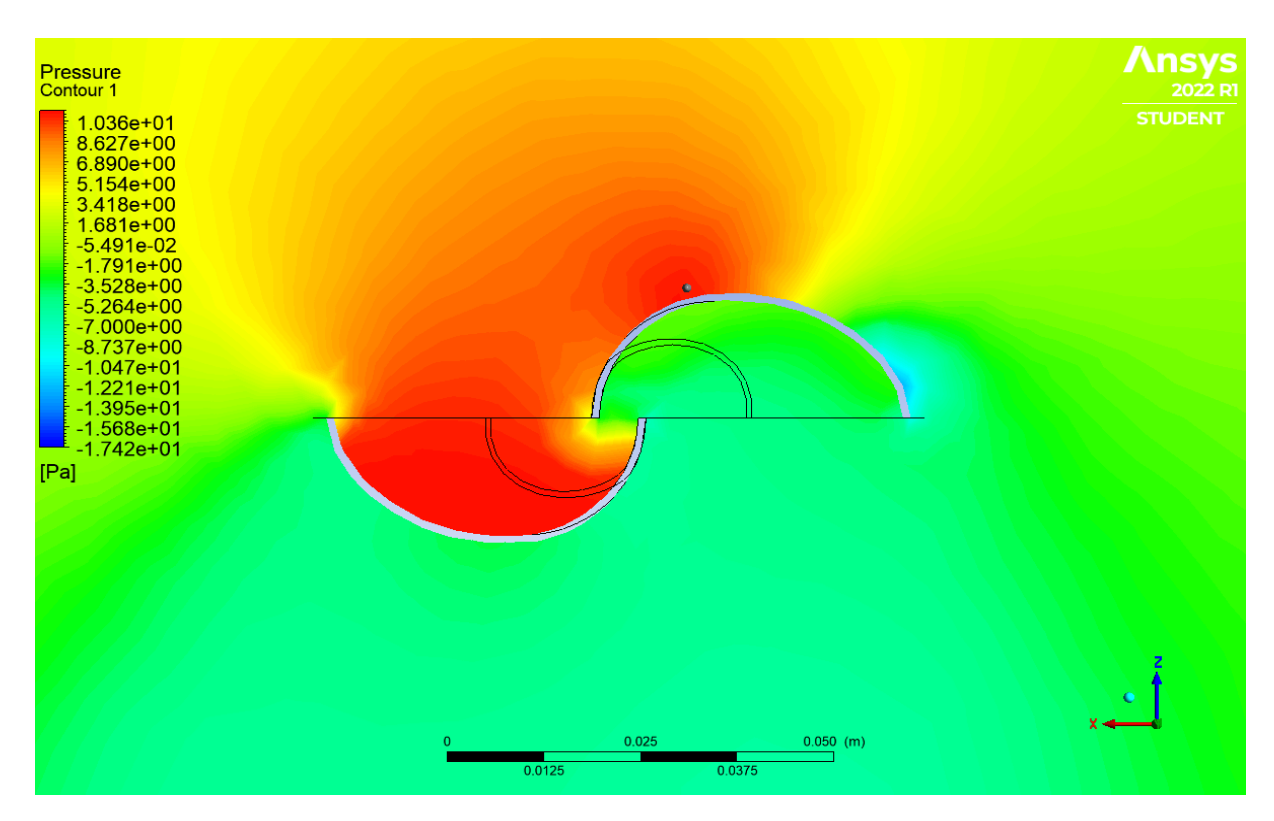


Figure 15. Pressure contours for optimized model

- 2. The angle between the tangent line and a lateral horizontal line is dimensionalized and parameterized in Ansys Design Modeler or SpaceClaim
- 3. Create an output parameter for the coefficient of moment in the Fluent window.
- 4. In the design parameters tab of the workbench, make multiple design values of parametrized angle.
- 5. Get plot for Cm versus the angle parametrized.

#### 8.2 Results

We considered a quadrant region for the angular range, and the maximum moment resulted at an overlap end spline angle of close to 90 degrees with the lateral line. Whereas, the moment increased gradually with acute angle of spline, and is constant after 70-80 degree range. The optimized model, with these spline angles is shown in the figure below,

The velocity and pressure contours show that there is significant improvement in flow, and the pressure difference between the returning blade is reduced. On the other hand, keeping the number of seed points and enclosure of the same specifications, the

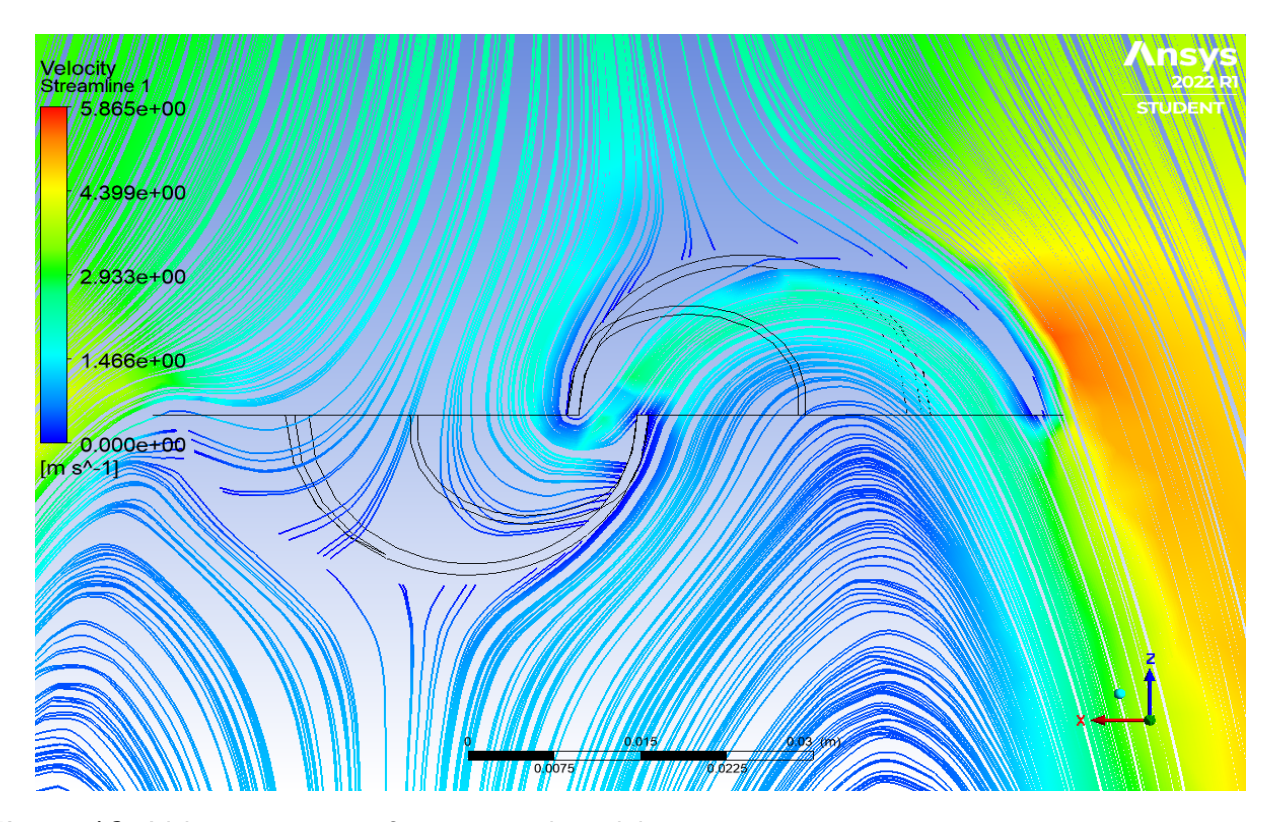


Figure 16. Velocity contours for optimized model

number of streamlines hitting the open blade has increased. The coefficient of moment for the optimized turbine is 0.31 which is a significant improvement in performance.

## 9 Experimentation

The industrial wind tunnel of Flow Control and Turbine Research Laboratory, Department of Mechanical and Industrial Engineering was used for the experimentation. The schematic diagram of the wind tunnel is shown in the Figure.18. The maximum speed of the tunnel is approximately 15 m/s or 54 km/h. The rectangular test section dimensions are of 60cm X 60cm. The wind tunnel was calibrated prior to the experiment.

Experiments were done to measure the power generated and rpm of the wind turbine. The power generated was evaluated using Dynamo and multimeter, whereas the rpm was measured using a tachometer. Further, the rake or velocity profile along a vertical line downstream of the turbine was plotted with the help of a pitot tube. This velocity profile is used to calculate the coefficient of drag acting on the turbine using the wake rake method.

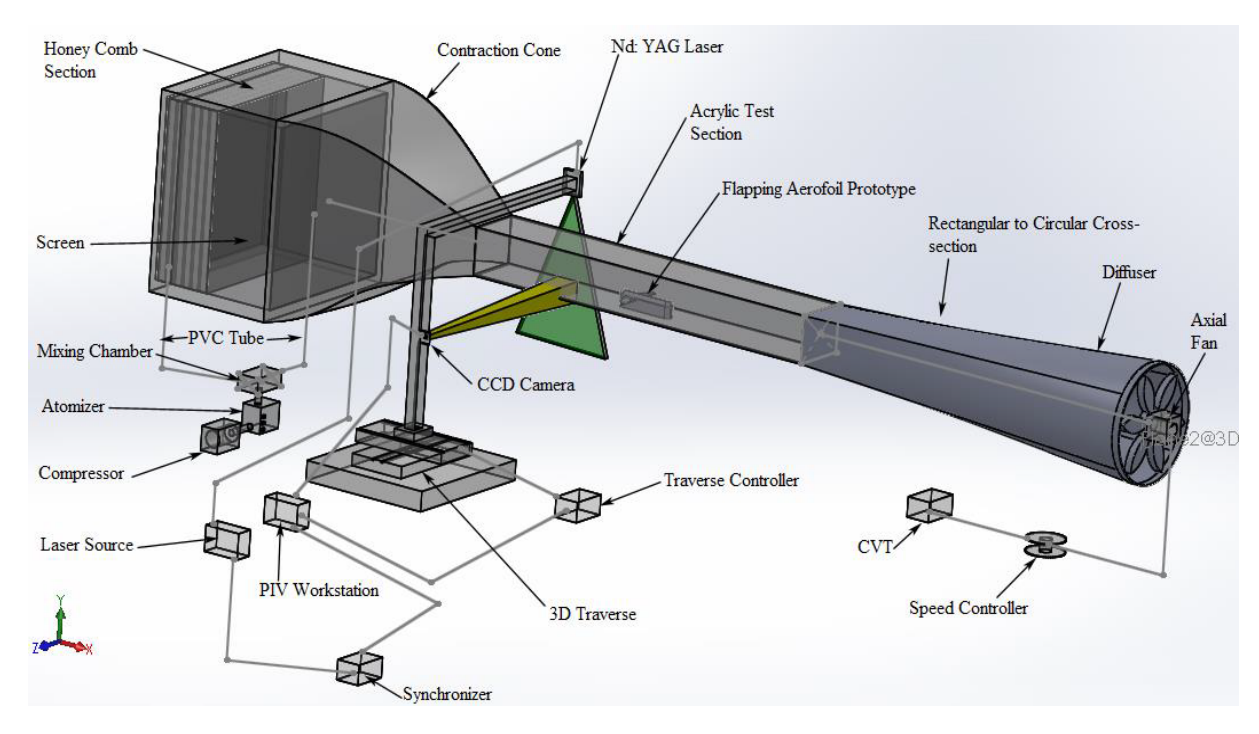


Figure 17. Schematic of wind tunnel at Flow-CTRL

#### 9.1 Prototype

The CAD model that we designed earlier was 3D printed in the Tinkering lab, IIT Roorkee using Delta Wasp 2040 3D printer which uses the Fused Deposition Modelling i.e. FDM technology. The material used for the prototype was Polylactic Acid (PLA). The model was printed at a nozzle temperature of 200°C at a print head travel speed of 220mm/s. The layer resolution was kept constant at 50 microns and the filament diameter was 1.75mm. The height of the SSWT is 23cm and the diameter is 9.4cm The prototype thus modelled was carried to the flow control and turbine research laboratory for wind tunnel testing.

## 9.2 Wind Tunnel Setup

The prototype along with the shaft was attached upside down to the top plate of the tunnel as shown in Figure.19. A bearing containing fixture is placed over the tunnel through which the shaft was passed and connected to the dynamo.

#### 9.3 Results

For the first experiment, the air velocity was varied to find the starting speed for the turbine blades. The wind turbine blades started rotating at the wind speed of 3m/s

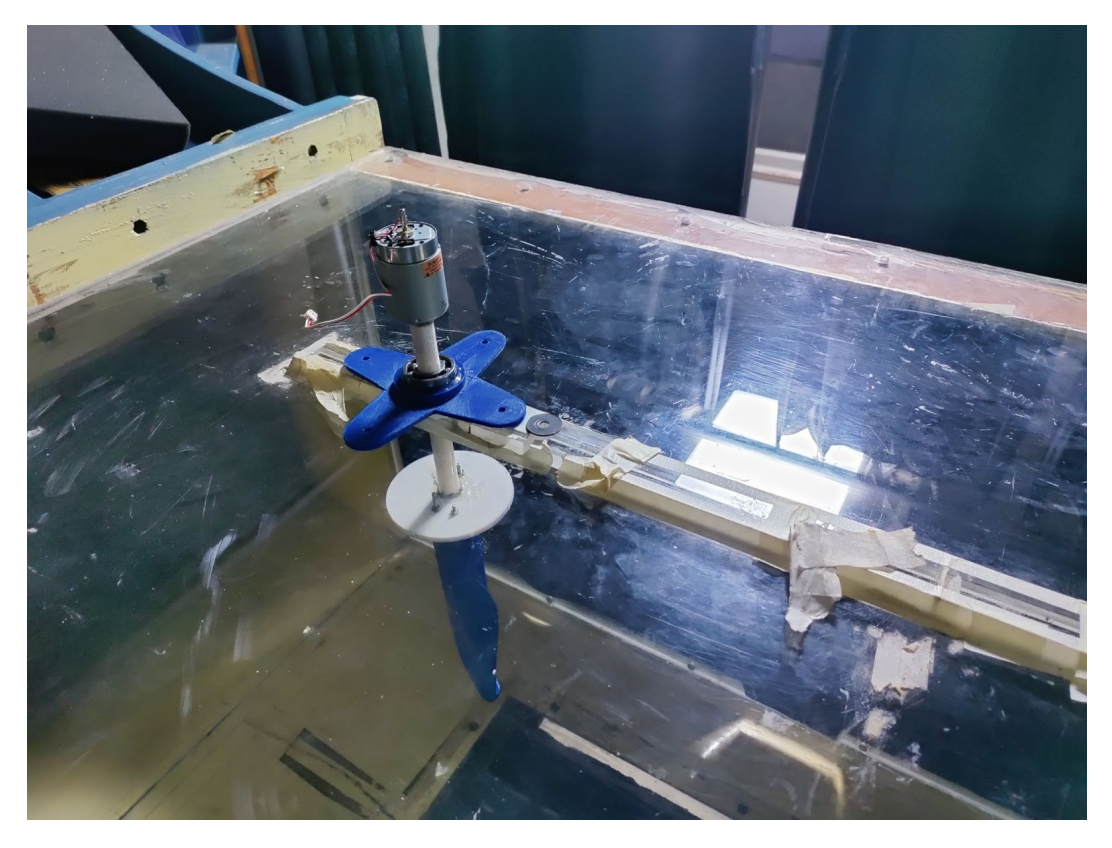


Figure 18. Fixture of turbine to wind tunnel from top-side view



Figure 19. Person measuring turbine rpm using tachometer

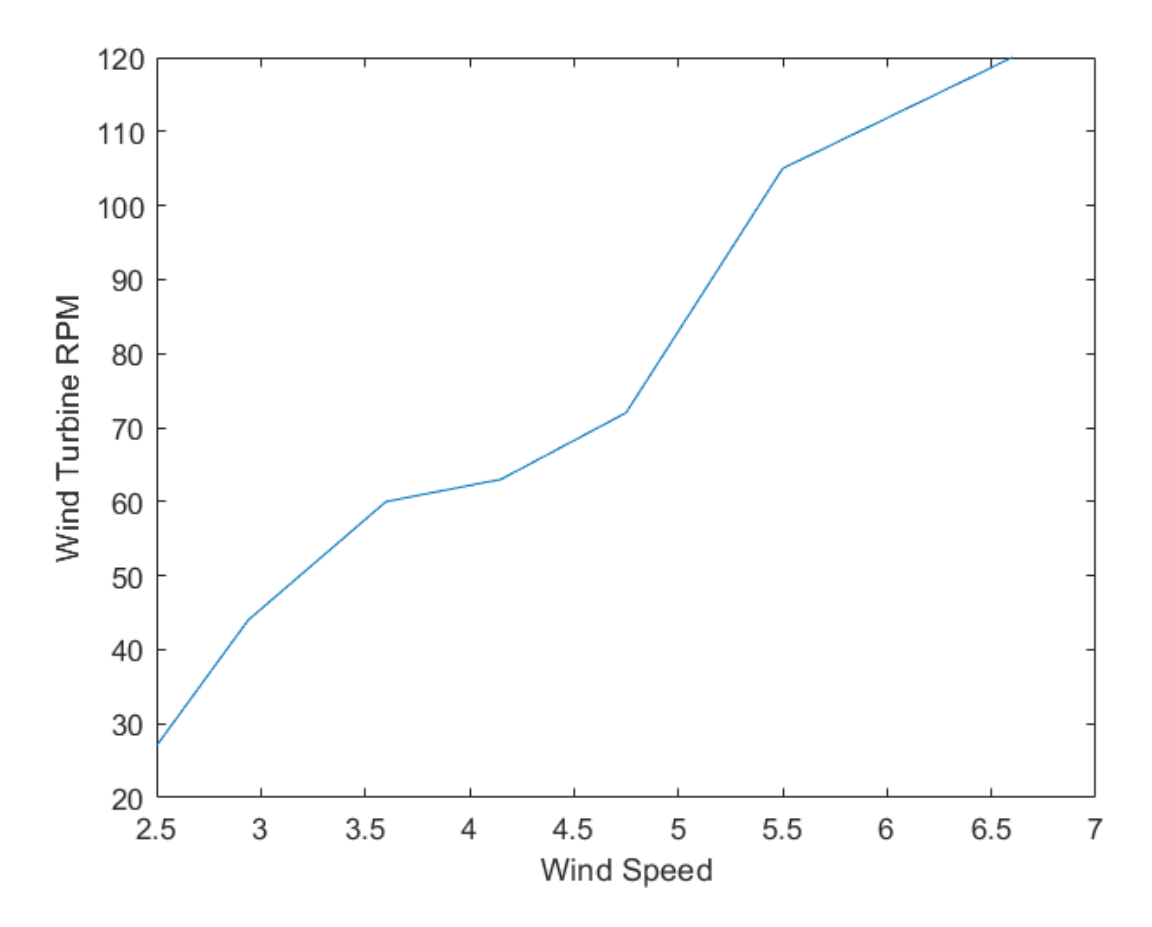


Figure 20. Wind Turbine rpm variation with wind speed in tunnel

or 10.8 km/h. The readings were observed for various wind speeds of the tunnel and they are plotted against the corresponding wind turbine rpm in the following graph (Figure.21)

Furthermore, the multimeter readings were also taken into account for the voltage difference produced against the corresponding wind speeds inside the tunnel. The same is also plotted in Figure.22. The voltage difference between the ends of the dynamo was observed to be increasing with increasing wind speeds. To calculate the drag coefficient, wake rake method was used. A brief description of the method is given below.

#### Wake Rake Measurement

When an obstacle is placed in flow, the flow gets disturbed due to the viscous effects. Consider a body placed in a wind tunnel and assuming specific control volume

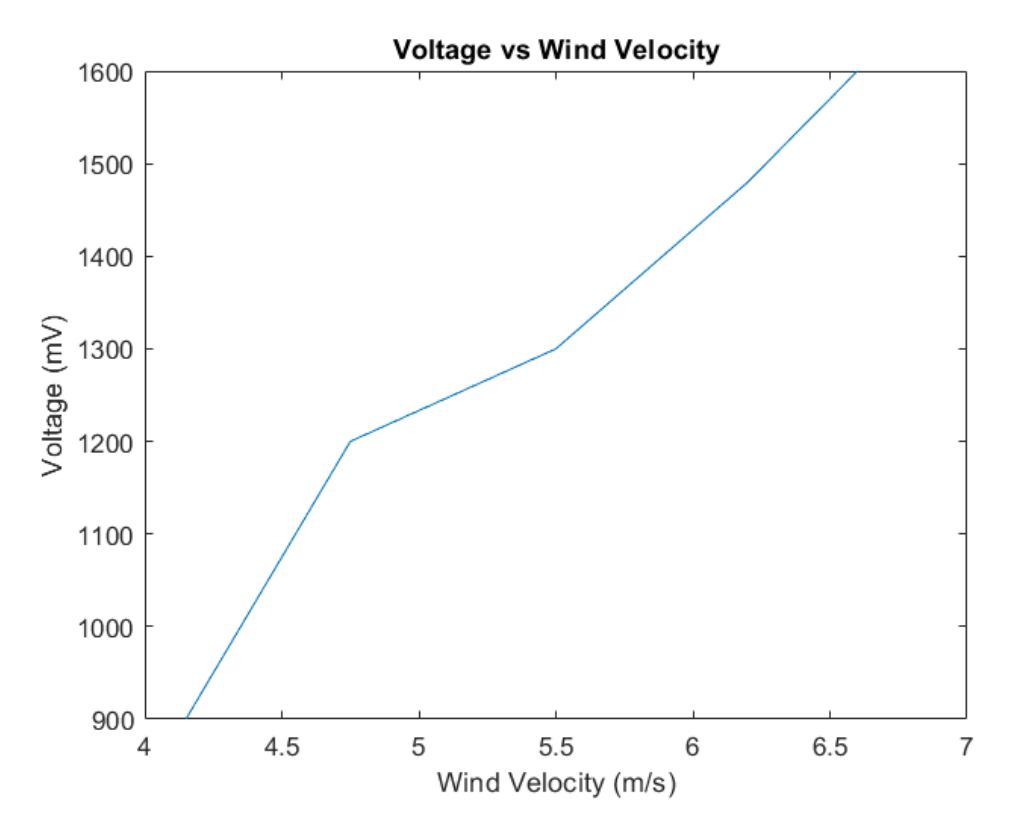
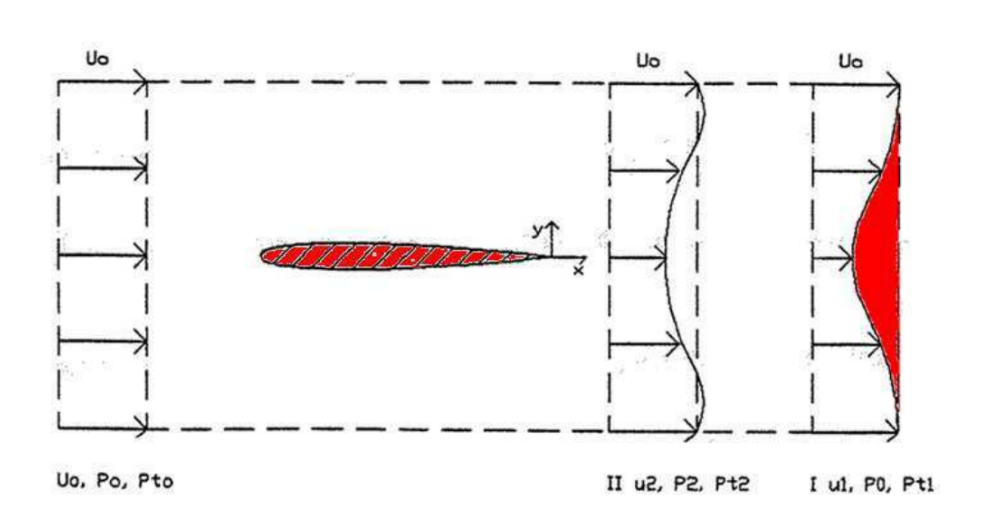


Figure 21. Voltage difference generated vs wind speed in tunnel

as shown in figure... At position 2 the velocity at centerline is close to zero because of obstruction, but as we move to position 3, the velocity profile gets developed.



**Figure 22.** Control volume with obstacle/body, velocity profile at tow positions

At this point, from the velocity profile it is clearly evident that the velocity is reduced near the centre due to the drag. Thus, from Newton's Second law, the momentum deficit in flow between

position 1 and position 3 is caused by the drag force. This method of calculating drag force is called wake-rake measurement. Assumptions in this method:



Figure 23. Setup for measuring pitot readings to get velocity profile (Rake)

- 1. Flow is steady
- 2. Incompressible flow
- 3. Static Pressure is same throughout the tunnel.

By solving continuty and momentum deficit equations, we get,

$$DragForce, D = \rho LU^{2} \int_{0}^{w} (1 - u^{2}U^{2}) dy$$

Coefficient of Drag, 
$$C_d = \frac{D}{\frac{1}{2}\rho U^2 S}$$

In the experiment, we placed the probe at a distance of  $\approx 10D$  and is vertically advanced to get pressure and velocity values at each location. The setup while carrying out the procedure is shown in Figure.24. The vertical fixture is connected to a scale, through which we note the depth of probe, whereas the velocity is measured through a digital manometer. A MATLAB code was written and executed for solving the expression, and the coefficient of drag came out to be 1.61.

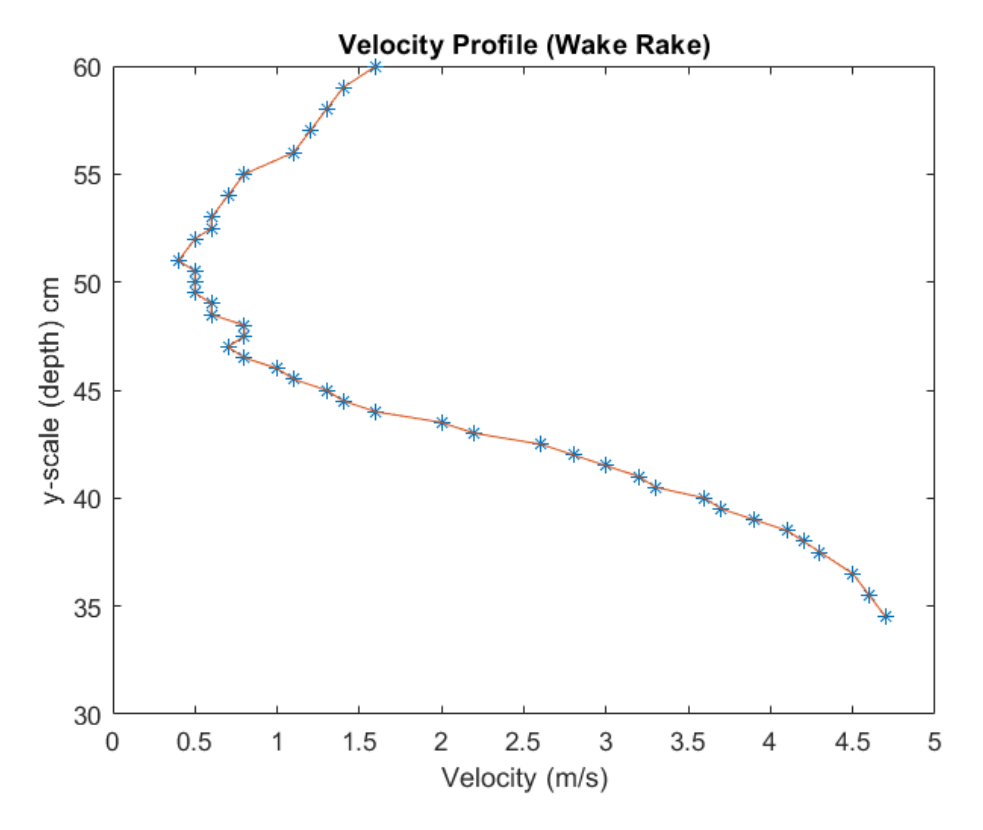


**Figure 24.** Velocity profile with y-scale on y-axis, at y=60cm the proble at the top most surface

#### 10 Gust Protection Mechanism

Since, the wind turbine is aimed for harnessing the low wind speeds in the range of 2-5 m/s, there were obstacles of how the wind turbine will cope up against strong wind forces or gusts. For that we designed a gust protection mechanism. Two good workable ideas were selected after brainstorming, and one was finalised and presented below. The first idea has an enclosure which moves linearly up and down upon detecting gust. The second one actuates the turbine which in turn activates the protecting shield using screw jack type mechanism. The second design is the finalised one as it provides no hindrance to the other blades (imagine the wind tree scenario) due to the inline arrangement of shields in the off gust conditions. As soon as the electric sensor detect the gust, the motor actuates the screw which upon pitching converts to linear motion of turbine. Additionally, a enclosure of cylindrical shape is deployed as the turbine moves linearly down. The detailed dynamic animation is shown in below pictures,

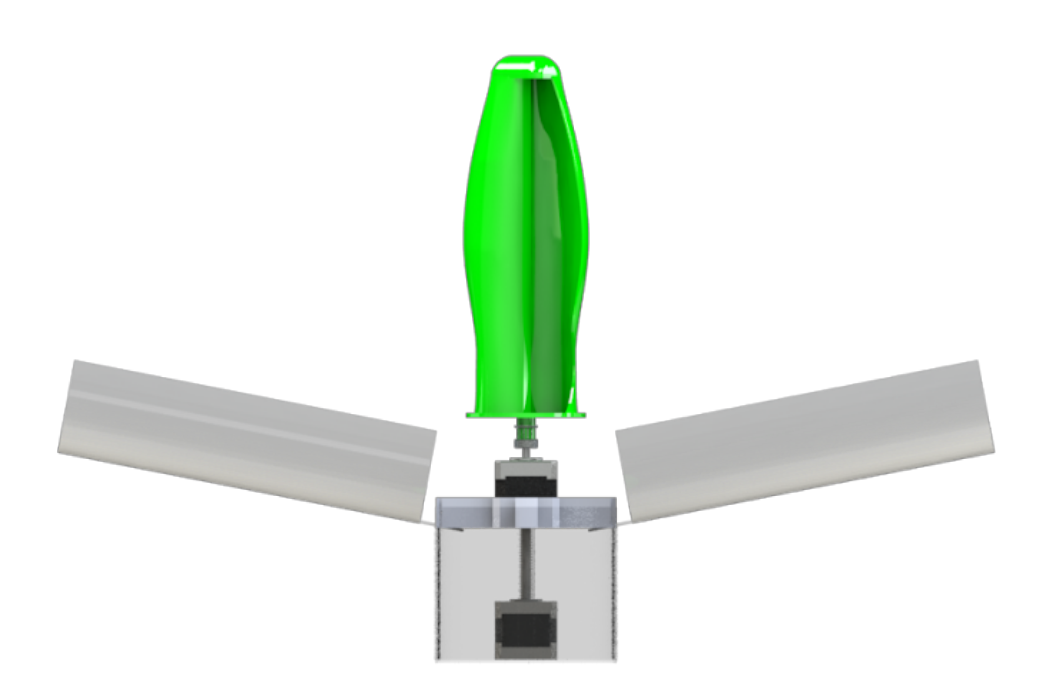
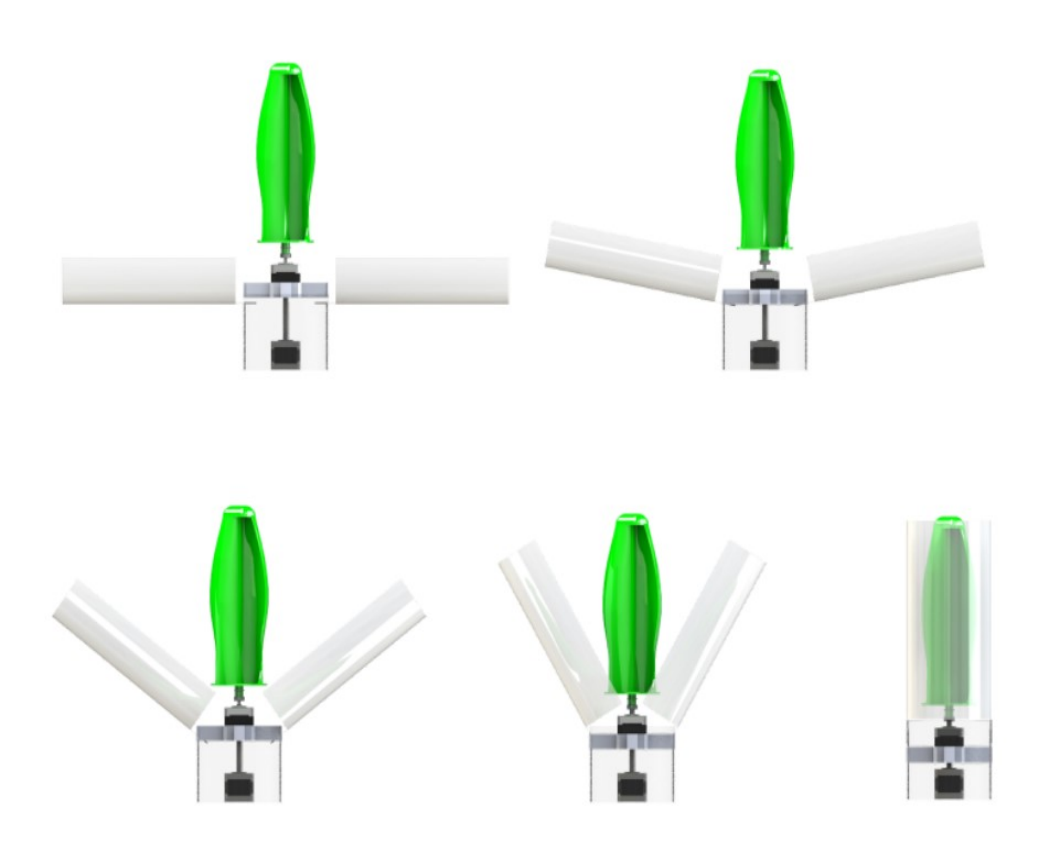


Figure 25. Gust Protection Idea-2



**Figure 26.** Z-wise, closing of turbine as the bottom motor pulls the turbine downwards.

## 11 Scaling wind turbines

Throughout the project, the main wind turbine model is scaled multiple times to meet the laboratory requirements. So, the performance variables such a torque, power also changes with scaling. The following table shows the effect of scaling and scales for each parameter,

Power	$\sim R^2$
Torque	$\sim R^3$
Angular Speed	$\sim R^{-1}$
Aerodynamic Forces	$\sim R^2$

### 12 Conclusion

The SSWT is thoroughly examined by numerical and experimental procedures. A number of design modifications were performed to get the final optimised model. Parametric optimization on AR (Aspect Ratio) of the blade suggests that AR of 2.32 and above gives the best results as proved from the Cm values in the static analysis. Spline optimization resulted in much better aerodynamics around the tip and overlap regions. The initial  $C_m$  0.27 is significantly increased by 15% to 0.31 through spline optimization. The experimental results proved that the turbine is best suited for low wind speed applications, as it starts rotating from 3 m/s velocities. However the wind speeds in the cities are still lower. So to cater those areas, it is required to further cut down the starting speed by limiting the friction in the assembly. Voltage vs wind speed plot shows that higher the speed, higher would be the power output (as we know, P = V2/R and R, being the resistance of the multimeter, is a constant throughout the experiment, so P  $\alpha$   $V^2$ ). The effect of drag in the turbine is clearly visible in the Cd value which comes out to be 1.61.  $C_d$  value greater than 1 implies the dominance of drag effect on the turbine. Finally a mechanism to protect the turbine blades from gust conditions is proposed as per the objectives.

## **Future Scope**

- 1. Spline Optimization can be extended to vary multiple parameters in different planes at a time.
- 2. Printing the exact model size rather than scaling down, to get the exact specifications.
- 3. In the experimental setup, proper gearing system can be installed to reduce load on turbine. Additionally, the friction in experimental setup can be reduced by proper joining and fixing processes.
- 4. Velocity profiles can be read along the plane in wake region to get accurate  $C_d$
- 5. Gust Control Mechanism can be prototyped and tested by creating gust conditions in wind tunnel.

### 13 References

- El-Ali, A., Moubayed, N. Outbib, R., Comparison between solar and wind energy in Lebanon. Proc. of 9th Int. Conf. on Electrical Power Quality and Utilisation, Barcelona, 2007.
- 2. Robert Whittlesey, Chapter 10 Vertical Axis Wind Turbines: Farm and Turbine Design, Wind Energy Engineering, Academic Press, 2017, Pages 185-202
- 3. Fujisawa, N., Gotoh, F., 1992. Visualisation study of the flow in and around a Savonius rotor. Exp. Fluids 12, 407–412.
- 4. Kunio, I., Jitendro, N.R., 2007. Characteristics of wind power on Savonius rotor using a guide-box tunnel. Exp. Therm. Fluid Sci. 32, 580–586
- 5. Altan, B.D., Atılgan, M.A., 2010. The use of a curtain design to increase the performance level of Savonius wind rotors. Renew. Energy 35, 821–829.
- 6. Golecha, K., Eldho, T.I., Prabhu, S.V., 2011. Influence of the deflector plate on the performance of modified Savonius water turbine. Appl. Energy 88, 3207–3217.
- 7. Abdulkadir Ali, Steve Golde, Firoz Alam, Hazim Moria, "Experimental and Computational Study of a Micro Vertical Axis Wind Turbine", Procedia Engineering, Volume 49, 254-262, 2012
- 8. Nobuyuki, F., 1992. On the torque mechanism of Savonius rotors. J. Wind. Eng. Indus. Aerodyn. 40, 277–292.
- 9. Mahmoud, N.H., EL-Haroun, A.A., Wahba, E., Nasef, M.H., 2012. An experimental study on improvement of Savonius rotor performance. Alex. Eng. J. 51, 19–25.
- 10. Dobreva, I., Massouha, F., 2011. CFD and PIV investigation of unsteady flow through Savonius wind turbine. Energy Procedia 6, 711–720.
- 11. Nasef, M.H., EL-Askary, W.A., AbdEL-hamid, A.A., Gad, H.E., 2013. Evaluation of Savonius rotor performance: static and dynamic studies. J. Wind. Eng. Indus. Aerodyn. 123, 1–11.
- 12. Scaling wind turbine and rules of similarity https://link.springer.com/content/pdf/10.1007%2F978-3-642-22938-1\_7.pdf

## **Image Sources**

- 1. https://en.wikipedia.org/wiki/Savonius\_wind\_turbine#/media/File:
   Savonius\_turbine.svg
- 2. https://en.wikipedia.org/wiki/World\_energy\_supply\_and\_consumption
- 3. http://www.alternative-energy-news.info/wp-content/uploads/2015/03/wind-turbine-tree-leaves.jpg
- 4. Measuring Wing Profile Drag using an Integrating Wake Rake Ellen A. Pifer, G"otz Bramesfeld Saint Louis University